International Journal of Automotive Technology, Vol. 15, No. 6, pp. 909–917 (2014)
DOI 10.1007/s12239–014–0095–6

pISSN 1229–9138/ eISSN 1976–3832

CRASHWORTHINESS DESIGN BASED ON A SIMPLIFIED DECELERATION PULSE

P. URBINA[1)*], P. ORTA[2)] and H. AHUETT-GARZA[2)]

[1)]Center for Innovation in Design and Technology, Tecnológico de Monterrey, Avenida Eugenio Garza Sada No. 2501, Monterrey N.L. 64849, Mexico
[2)]Department of Mechanical Engineering, Tecnológico de Monterrey, Avenida Eugenio Garza Sada No. 2501, Monterrey N.L. 64849, Mexico

(Received 6 February 2012; Revised 14 December 2012; Accepted 16 November 2013)

ABSTRACT–This paper proposes a procedure to improve the design of an automobile crashworthiness using the deceleration pulse in a simplified form as a design variable. A complete vehicle in a full frontal crash was simulated to find its deceleration pulse by finite element method. Based on this deceleration pulse, sled tests were performed, also in a virtual environment. Comparisons between the real deceleration pulse and a simplified pulse were made based on the HIC_{15} produced. The simplified pulse is developed by dividing the pulse in three phases, each with a constant level of deceleration. Simulations were made to minimize the HIC_{15} changing parameters in the restraint system and in the deceleration pulse. An expression was found to relate HIC_{15} and the first phase of the deceleration pulse. A design case using this expression is presented. The benefits of using the pulse as a design variable along with the restraint system are accounted.

KEY WORDS : Deceleration pulse, Crashworthiness design, Finite element simulation, Sled test

NOMENCLATURE

NHTSA	: National Highway Traffic Safety Administration
HIC	: Head Injury Criterion
FMVSS	: Federal Motor Vehicle Safety Standards
FMVSS 208	: Occupant Crash Protection regulation of the National Highway Traffic Safety Administration
IIHS	: Insurance Institute for Highway Safety
NCAC	: National Crash Analysis Center
NCAP	: New Car Assessment Program
TWB	: Tailor Welded Blanks
FE	: Finite element

1. INTRODUCTION

When a car impacts a barrier, the structure of the car is deformed in a characteristic way. The vehicle's kinetic energy is transformed into energy of deformation. The impact triggers the airbag and the occupant begins its movement forward. When a seat belt is used, the occupant movement is restrained. In about 30 milliseconds, the air bag deployment will reach its maximum level and will help reduce the kinetic energy of the person. As this happens, the vehicle continues its deformation as the structure protects passengers from dangerous intrusions in the cabin. The shock event ends at approximately 100 milliseconds after the initial impact.

There are several factors that affect the response of the car to the impact, such as the stiffness of the structure, damping, mass and interactions with the outside environment. An excellent indicator of the vehicle's response to the crash is the deceleration pulse, which defines the nature and severity of impact (Huang, 2002). Some authors consider that the deceleration pulse is the essential feature of the design process for crashworthiness (Du Bois *et al*., 2004).

The severity of a crash can be measured by the damage caused to its occupants. The head injuries are the leading cause of death and disability in humans, and about half of the head injuries are caused by car accidents (McHenry, 2004). The expected damage in the head has been characterized by the Head Injury Criterion (HIC_{15}) introduced in equation (1).

$$HIC_{15} = \max_{t_1,t_2}\left\{\left[\frac{1}{(t_2-t_1)}\int_{t_1}^{t_2} a_r\, dt\right]^{2.5}(t_2-t_1)\right\} \quad (1)$$

Where $(t_2–t_1)$ represent a period of 15 milliseconds selected to maximize HIC_{15}. Variable a_r represents the resulting acceleration measured in the head. Regulation FMVSS 208 (NHTSA, 2008) of the NHTSA establishes that in the event of collision, HIC_{15} must not exceed 700. IIHS also takes into account this criterion in assessing the

**Corresponding author.* e-mail: pd.urbina.phd.mty@itesm.mx

risk of head injury (Insurance Institute for Highway Safety, 2009).

This paper focuses on the use of the deceleration pulse shape for a vehicle crashworthiness design and analyzes its effect in the HIC_{15}. The objectives of this work include the analysis of:

- The implication of the use of the deceleration pulse in a simplified way and its deviation (in the HIC_{15} produced) from a real continuous pulse.
- The improvements in HIC_{15} in a frontal crash test, achieved by considering the deceleration pulse among the design variables during optimization of the restraint system (airbag and seat belt).
- The relationship between the injury criterion (HIC_{15}) and the shape of the deceleration pulse of a vehicle.

The results derived from this paper could be useful in the development of a more comprehensive methodology for the initial stages of crashworthiness design. The scope of this paper is limited to the analysis of full frontal crashes and a single objective injury criterion (HIC_{15}) measured in the vehicle driver position.

The section 2 reviews the previous works related to the deceleration pulse and its simplification in crashworthiness. Section 3 provides the process followed to obtain the finite element models used in the rest of this work. Section 4 shows the information of the proposed simplification of the pulse and accounts for its suitability in HIC_{15} predictions. Section 5 quantifies the improvements in HIC_{15} by using the pulse as a design variable in a simplified form. In section 6 a study case is presented. The remarks, conclusions and future work are reported in Section 7 and 8.

2. LITERATURE REVIEW

For the design of automotive structures, the aspect of safety is of superlative importance. Numerous papers that address the issue of safety, and which propose the use of the finite element method to achieve optimizations and improvements, can be found in literature (Xu *et al*., 2010; Lee *et al*., 2007; Wu and Xin, 2009; Fang *et al*., 2005). In some of these works, the approach followed is to modify the design of a component (or several) and measure changes in energy absorbed or developed peak force when subjected to impact.

To achieve the best solutions, several authors propose the use of topological and shape optimization techniques (Xu *et al*., 2010; Lee *et al*., 2007). However, these techniques are difficult to apply for the case of crashworthiness analysis, because they require a considerable number of variables. Under such circumstances, the total processing time can be very high (Patel, 2007). Other authors have used genetic algorithms combined with response surface methods. Table 1 compares several of these studies. An important conclusion can be derived from the table: with more design variables, a major number of runs is required.

(Cao *et al*., 2004) prepared a review that supports the division of an optimal deceleration pulse in 3 phases which is also explained by Witteman (2005). These 3 phases are defined as follows:

- Phase 1: In this first stage the collision is produced and the passenger starts his/her movement forward. Because there is no impact between the passenger and the interior of the vehicle during this phase, high deceleration of the vehicle can be allowed.
- Phase 2: The airbag expands and contact with the passenger begins. During this stage the vehicle deceleration should be kept low to reduce the amount of damage.
- Phase 3: Contact between passenger and airbag is fully developed. The airbag must perform its task and prevent potentially dangerous impacts and high decelerations in

Table 1. Optimization studies for crashworthiness, application of genetic algorithms and response surface methods.

Reference	Optimization methodology	Number of runs	Number of design variables	Nature of design variables	Number of objective functions	Nature of objective functions
(Chen and Li, 2009)	Response surface method (enhanced)	136	8	Thickness	1	Acceleration peak of B Pillar
(Hilmann *et al.*, 2007)	Monte Carlo + genetic algorithms	>100	15	Thickness and bumper section parameters	1	Plastic strain (minimize)
(Hamza and Saitou, 2005)	DOE + genetic algorithms	54	18	Sectional height and width (4), thicknesses (14)	2	Passenger compartment intrusion, maximum passenger point acceleration
(Fang *et al.*, 2005)	Response surface method	27	10	Thickness	3	Energy absorbed at 20 ms and 40 Ms and peak acceleration at engine top
(Wu and Xin, 2009)	Response surface method	12	3	Sectional height, width and angle of the S-Rail	1	Internal energy

the passenger's head and chest. The deceleration of the vehicle during this phase can be moderately high.

Witteman (2005) obtained the optimized deceleration pulses at 32, 56 and 64 km/h. According to his work, for a crash at 64 km/h, for phase 1 (first 18 cm of deformation), a deceleration of 45 g's is desirable. For phase 2 (frontal deformation between 18 cm and 59 cm), a deceleration of 9 g's is preferable. For phase 3 (a length of 59 cm of deformation to 76 cm), a deceleration of 23 g's is desirable. The duration of each phase is almost constant regardless of the initial velocity (Witteman, 1999), and corresponds to between 10 and 30 ms for the first phase and approximately 35 ms for the second phase.

With regards to the changes and structural improvements, it is very useful to implement a decomposition in time and space (Qi, 2008; Hu *et al*., 2009). This will limit the analysis as well as reduce simulation time and number of variables to modify. The decomposition time can be based on the phases explained before. The delimitation in space can be achieved by the choice of certain components that are important in the observed crash mode (Hamza, 2008).

In the work of Cao *et al*. (2004) an experimental design was conducted to identify the parameters of the restraint system (airbag and seat belt) that have the most important effects from the perspective of occupant damage in a frontal collision. Their results suggest that the force on the seat belt retractor and the area of the vent hole in the air bag are the most important parameters. Also, they proposed an optimization of the parameters of the restraint system along with the deceleration pulse as a design variable. This methodology differs from the "traditional approach" which first makes a structure as efficient as posible from the perspective of energy absorbed and then, the resultant pulse is introduced as an input in the restraint system optimization.

This work builds on the procedure proposed by Cao *et al*. (2004), who combined design of experiments with optimization of restraint system parameters along using the deceleration pulse. This work goes further by including the deceleration pulse among the design variables and quantifying the improvements obtained in the optimization of the resulting HIC_{15}.

The pulse divided into three or more phases of constant deceleration, represents a simplification of the pulses obtained in real life. However, the works cited previously do not provide a measure of the error or deviations incurred by making this simplification. The present study tests the simplifications of the deceleration pulse and analyzes its effect on HIC_{15}.

The 40% offset crash test (Figure 1) is an important test included in FMVSS 208 and used by the EURONCAP (EURONCAP, 2011) and the IIHS (Insurance Institute for Highway Safety, 2009). However, some documents state that in the full frontal crash test major damage is produced by head and chest decelerations (Kawabe *et al*., 2004) and this test is the best to prove restraint systems (Griffiths *et al*., 1999). For this reason, this work focuses in the full frontal crash test only.

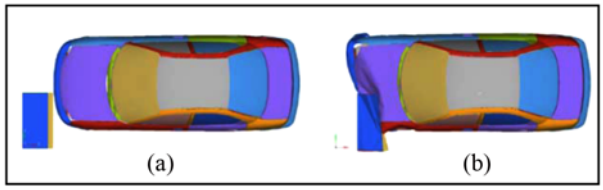

Figure 1. Top view of the 40% offset crash test.

3. DEVELOPMENT OF FE CRASH MODELS

Complete standardized FE meshes were obtained from specialized sites. A complete vehicle model that includes the mesh, material characterization and rigid wall, was obtained from the NCAC's website (Opiela, 2010). The FE models that can be found in this website have been used by various authors in other research, for example (Consolazio *et al*., 2003; Goel and Stander, 2009). Also, FE models were used to simulate test dummies obtained from LSTC®. These components were integrated within HYPERMESH® pre-processor software and were solved through LS-DYNA® finite element software. The results were visualized with the softwares HYPERVIEW® and LS-PREPOST® (for the case of the calculation of HIC_{15}).

The FE model of the complete vehicle that was used corresponds to a vehicle DODGE NEON 1996 with 270,768 finite elements, mostly shells (Figure 2). A more detailed description of the model can be found in (Solanki *et al*., 2004).

A frontal crash test was simulated at 35 miles per hour. The velocity was compared with experimental data of the NCAP and other virtual simulation presented in the NCAC report (NCAC, 2006). Results are shown in Figure 3, where as expected, the plots are very similar.

To obtain the HIC_{15} by means of different deceleration pulses, sled test simulations were conducted. In sled tests, only the models of the cabin and the driver were used. When applying a deceleration pulse to the cabin, the HIC_{15} produced in the driver was recorded.

In the simulations of the sled tests, the whole cabin was modeled. In particular, the airbag was simulated by a

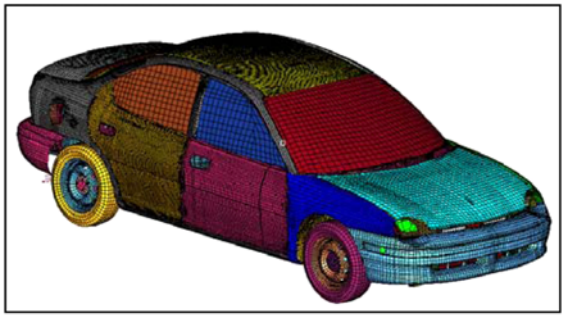

Figure 2. FE model used in this work.

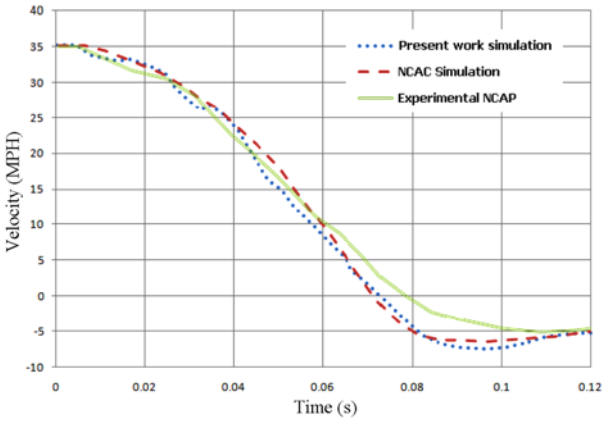

Figure 3. Comparison of the velocity history of the experimental test, the NCAC simulation and the present work simulation.

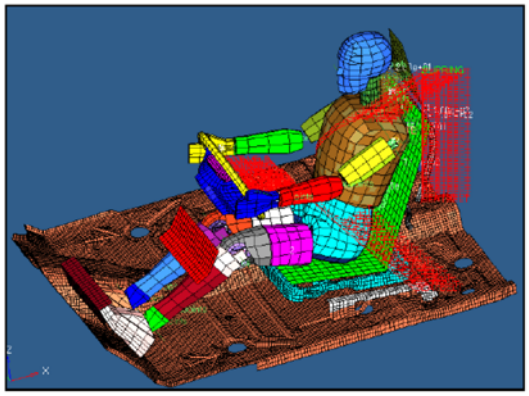

Figure 4. Driver cabin model with positioned dummy.

control volume (also obtained from NCAC website). The seat belt was represented by one dimensional elements in contact with the dummy model of a man of 50 percentile (Figure 4). The dimensions of the cabin are based on (Macey and Wardle, 2009).

4. DECELERATION PULSE SIMPLIFICATION AND HIC_{15} DEVIATION FROM ACTUAL PULSE

As mentioned in Section 2, the deceleration pulse can be broken down and simplified into discrete phases or levels. Simplification of the deceleration pulse is necessary because it allows its use as a design variable (Cao *et al.*, 2004). However, simplified models can produce deviations in the results as compared to predictions made based on full models.

As explained before, this work compares the results of a simplified model of deceleration pulse versus those produced by the full continuous deceleration pulse, based on HIC_{15}. In the simplified model, the actual deceleration pulse obtained by the full frontal crash test was divided into 3 phases. Each phase corresponds to the time spans during the deceleration pulse identified by Witteman (1999; 2005) as presented in Section 2. The first phase accounts for the initial 18 ms, the second phase lasts from 18 ms to 58 ms, and phase three ranges from 58 ms to the time for zero speed (72 ms). The deceleration is modeled as a series of steps, whose magnitude is the average of the real deceleration recorded at each stage. For phase i, the deceleration level (aL_i), can be obtained from equation (2), where $t1$ is the time at which the phase starts, $t2$ is the time at which the phase ends and a is the deceleration pulse of the vehicle.

$$aL_i = \frac{\int_{t1}^{t2} a \cdot dt}{t2 - t1} \tag{2}$$

This parameter aL_i represents the deceleration in each phase with a single value. Also, the change in velocity for each level remains unaltered. The underlying assumption here is that the deceleration peaks presented occur so rapidly that the system is unable to respond, and therefore its effects within each phase are not directly transmitted to (or "felt" by) the driver's head. Instead, the authors' hypothesis is that an average deceleration in each phase, can represent the damage caused by the real deceleration pulse.

To support the assumption, an initial full frontal crash test was simulated. The deceleration levels for each phase in the simplified form of the pulse resulted in 5.7 g's (first phase), 32.0 g's (second phase) and 32.9 g's (third phase). A comparison of the real pulse and the simplified form of the pulse is shown in Figure 5.

Damage predicted by the simplified model was compared to damage produced by the real deceleration pulse with runs of the sled test simulations. Different levels in the restraint system parameters were used. The comparison is shown in Table 2 and the deviations (d) were calculated using equation (3).

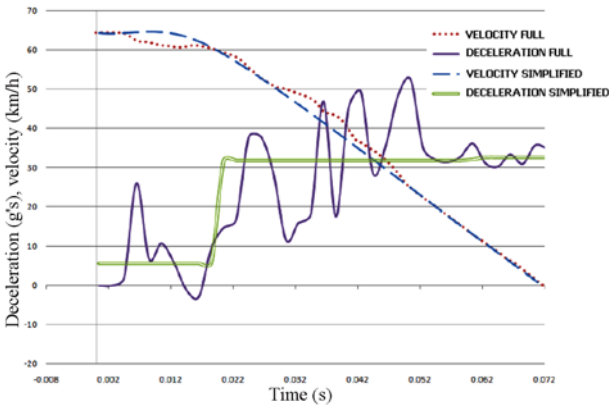

Figure 5. Comparison between the real pulse and the pulse simplification to the time to zero.

Table 2. Comparison of the HIC15 for the real deceleration pulse and the simplified version of the deceleration pulse. Fr= Retractor force, VAA=Vent hole area of airbag.

Nivel de parámetros	HIC_{15} real pulse	HIC_{15} simplified pulse	*d*
Fr = 4500 N, VAA = 400 mm²	1062	1193	12.33
Fr = 4500 N, VAA = 800 mm²	1787	1535	14.1
Fr = 4500 N, VAA = 1200 mm²	1542	1666	8.04
Fr = 8000 N, VAA = 400 mm²	520.8	523.1	.44
Fr = 8000 N, VAA = 800 mm²	394	421	6.85
Fr= 8000 N, VAA = 1200 mm²	352	359.2	2.04

$$d = \frac{HIC_{15\_REAL\_PULSE} - HIC_{15\_SIMPLIFIED\_PULSE}}{HIC_{15\_REAL\_PULSE}} \cdot 100\% \quad (3)$$

The results show that for values of HIC_{15} under 512, the deviation is relatively low (around 3.12% on average) and it increases as the value of HIC_{15} increases above 1062 (average deviation of 11.4%). The deviations are relatively small. The correlation coefficient between the two sets of data is of .975 for this particular case. This means that one set of data, in this case the HIC_{15} obtained by the real pulse, can be related with the other set of data, in this case the HIC_{15} obtained by the simplified pulse, with reasonable accuracy for the ultimate purposes of analysis and design. As explained before, this simplified form facilitates the introduction of the deceleration pulse shape as a design variable in the sled tests. The sections that follow will illustrate the procedure to do so.

5. SIMPLIFIED PULSE AND OPTIMIZATION OF RESTRAINT SYSTEM BY FACTORIAL DESIGN AND RESPONSE SURFACE

5.1. Optimization of Restraint System: Traditional Approach

To establish a frame of reference, a design exercise in the traditional approach was elaborated. Simulations of the sled test aimed at minimizing the value of HIC_{15} were conducted. In the reference case, the design parameters of the restraint system (force in the seat belt retractor and area of the vent hole in the airbag) were varied. The actual deceleration pulse of the FE model simulated at 64 km/h (full frontal crash against a rigid wall), as shown in Figure 5, was used as an input.

Table 3 shows the results and the values assigned to the design variables A (force in the seat belt retractor) and B (area of the vent hole in the airbag). The design space is explored using a factorial design 3^2. Because the best value of HIC_{15} was located in one of the extremes, 3 simulations were added around it.

As seen in Table 3, the behavior of HIC_{15} is much higher than 700 for low values in the force of the seat belt retractor. By increasing the force on the retractor to 11,500 N, HIC_{15} is improved to its lowest value; however, the deflection in the chest becomes very high. In the case of a force on the retractor of 8,000 N, this force may still be too high. For this level of force, there is a risk of injury which increases with age of the passengers, according to literature (Yannaccone *et al*., 2005).

5.2. Optimization of Restraint System: Using the Deceleration Pulse in a Simplified Form

An alternate design methodology, which uses the deceleration pulse as a design variable, was developed in a second group of simulations of sled tests. To make the problem tractable, the deceleration pulse was introduced using the three stages model explained in the Section 4. With the simplified model, the deceleration level in the first 2 phases is added to the design variables. The time to zero velocity remains in 72 ms.

To find the most important factors, a fractional factorial design of resolution IV (4 factors, 2 levels) was carried out.

Table 3. Results of the sled test in HIC15 and chest deceleration for different levels in A) retractor force of the seat belt and B) vent hole area of the airbag.

A\B	400 mm²		800 mm²		1200 mm²		1600 mm²	
	HIC_{15}	Chest deflection (mm)	HIC_{15}	Chest deflection (mm)	HIC_{15}	Chest deflection (mm)	HIC_{15}	Chest deflection (mm)
1000 N	2355	80	2173	75	1664	70		
4500 N	1062	65	1787	58	1542	45	1587	40
8000 N	521	47	394	45	**352**	**45**		
11500 N			277	65			280	65

The parameter to minimize is again HIC_{15}.

The design variables considered are:

A. Force in the seat belt retractor (1000–4500 N)
B. Area of the vent hole in the airbag (400–1200 square mm)
C. Level of deceleration in the phase 0–18 ms (5–50 g's)
D. Level of deceleration in the phase from 18 to 58 ms (5–50 g's)

Again, note that the deceleration is characterized by two values only. A full model of the deceleration spectrum would require more parameters, to the point that it is impractical to use as a design variable. Figure 6 shows that the effect of design variables C (deceleration level from 0 to 18 ms) and A (force on the retractor) stand out clearly. For optimization, the variables B (vent hole in the airbag) and D (level of deceleration from 18 to 56 ms) were taken as constants with values, for B = 800 mm^2 and for D = 9 g's.

For the optimization, design variables were redefined:

A. Force on the retractor (1000–4500 N)
B. Level of deceleration in the Phase 0–18 ms (5–50 g's)

To perform the optimization, a central composite design of 2 factors is chosen. The design required 9 runs. The design of the experiment was conducted with the help of MINITAB® software. The results are shown in Figure 7.

It is clear that increasing the force on the retractor can deliver better HIC_{15}. A force beyond 4500 N in the retractor was not explored because of the mentioned risk in chest damage. For the optimal level of deceleration in the first 18 ms, the full quadratic model (metamodel) obtained from the response surface is used as introduced in equation (4):

$$\begin{aligned} HIC_{15} &= 3368.10 - 0.303099 \cdot B - 92.3867 \cdot A \\ &+ 1.17539\text{E}-0.5 \cdot B \cdot B + 0.857750 \cdot A \cdot A \\ &+ 0.00290382 \cdot B \cdot A \end{aligned} \quad (4)$$

For equation (4), B is the level of deceleration and A the force of the retractor. The optimum value of HIC_{15} is placed on the retractor at its maximum force and the level of deceleration in the first 18 ms at 46.2 g's. The minimum HIC_{15} obtained was 408.4.

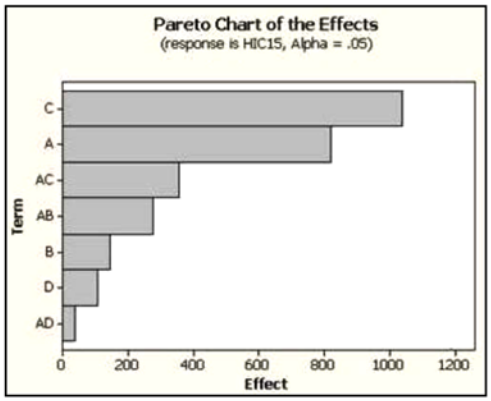

Figure 6. Pareto Chart with the effects in HIC15 of the most important design variables.

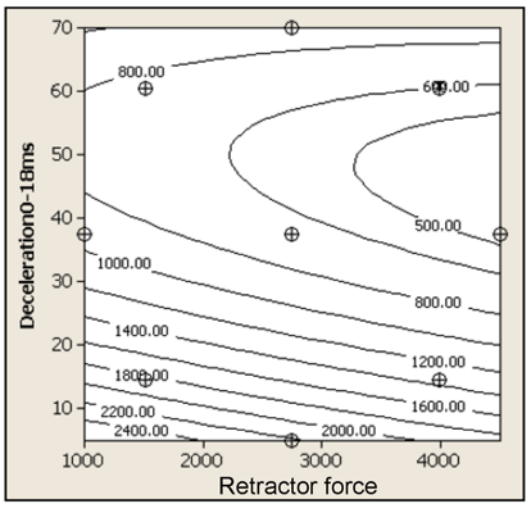

Figure 7. Contour plot of the values obtained for the HIC_{15}.

The quadratic model closely predicts the results of the test sled. When reproducing the sled test with optimal levels in the parameters, a HIC_{15} of 394.4 was obtained (3.56% error compared to the quadratic model). For levels of deceleration of the original structure, with a vent hole area of 800 square mm and force in the retractor of 4,500 N, the quadratic model reports a value of 1820.52 (compared to 1788 obtained by the sled test).

The optimal level of deceleration for HIC_{15} obtained for this first deceleration phase of 46.2 g's, matches values reported in literature by Witteman (2005) whose study locates it at 45 g's.

6. DESIGN CASE: APPLICATION OF THE METAMODEL IN THE FIRST PHASE OF DEVELOPMENT OF A CRASH TEST SIMULATION

From the results of the previous section, it can be seen that there is a considerable difference between the level of deceleration for the first phase of the crash as suggested for the optimization procedure (46.2 g's), versus the actual (5.7 g's). To reduce the risk of injury of the vehicle´s occupants, the next step would be to modify the structure of the car to produce a deceleration value closer to the optimum. In this case, changes in the structure of the car are explored, specifically, to the rails or side members (S-rail) shown in Figure 8. Rails have an important role in the initial development of the crash mode as can be seen in Figure 9, where the crash mode and global bending deformation of these members in the first phase is evident.

The structural changes that are explored in the simulations are based on common structural modifications found in studies of crashworthiness and energy absorption. The structural changes explored were:

Type 1 - Changes in thickness in S-Rail and division in

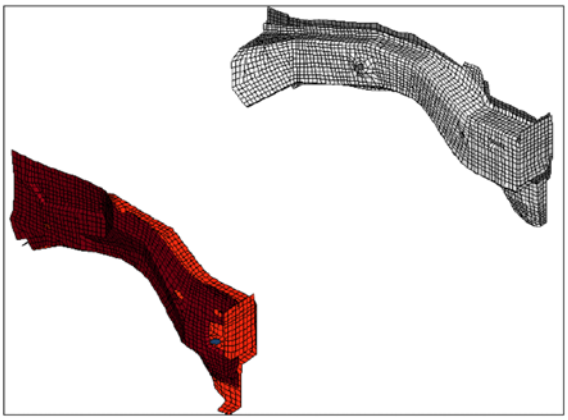

Figure 8. Side rail members.

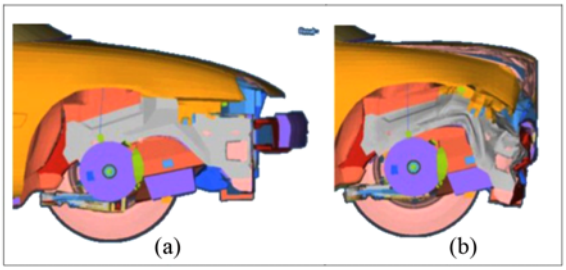

Figure 9. Deformation mode of the first phase of the crash.

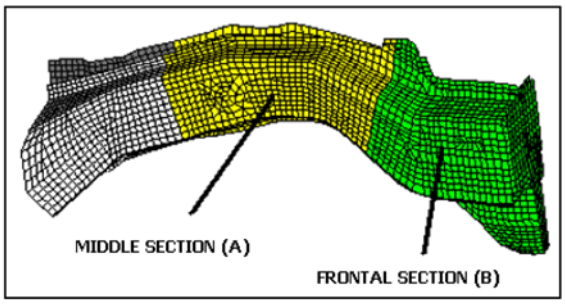

Figure 10. Division of the side rail member. Each section is simulated with a different thickness.

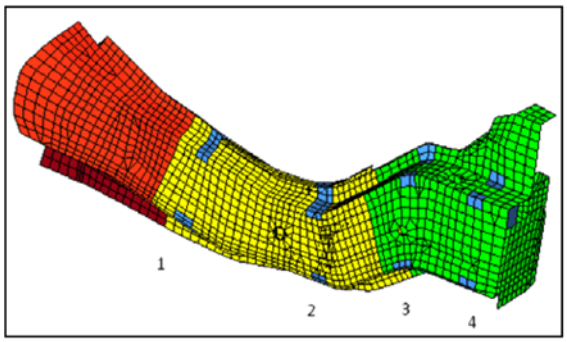

Figure 11. Side rail member with 4 crush initiator zones. The numbered zones contain elements with a smaller thickness (.75 mm) to represent weakened areas.

TWB: Each rail was broken into 3 sections similar to the study of Shi *et al.* (2007) as shown in Figure 10. The design variables to analyze were the thicknesses of each section, which could take the values of 1.5 or 3 mm.

Type 2 - Changes in thickness and material (yield strength) with not TWB divisions: The metal sheet thickness levels for the whole S-Rail used were 2.5, 3 and 3.5 mm. Levels of yield strength were 400 MPa and 800 MPa (simulating steel and high strength steel).

Type 3 - Adding crush initiators: Weakened areas (elements of .75 mm of thickness) used to initiate the deformation were placed on the rail (3 mm of thickness) with the objective of gaining some control of the crash mode. Structural modifications with the objective of control of the initial peak force and the subsequent deformation can be found in (Eren *et al*., 2009) and (Xu *et al*., 2010). Three configurations were tested with 4, 5 and 8 crush initiators zones. Figure 11 shows the first of them.

For the 3 types of structural modifications, the mesh is the same as the original model used in the last sections and changes were applied locally in the properties and materials of the shell elements affected in each case. The crash analysis corresponds to a full frontal crash against a rigid wall at 64 km/h.

Time decomposition is proposed to analyze only the first 40 ms of the crash under the premise that, as seen in the previous section, the first phase of the crash is of great importance for the HIC_{15}. A prediction of the HIC_{15} is proposed based on the equation (4). It should be noted that this equation depends on the simplified or average

Table 4. Potential HIC15 prediction based on the results of structural changes simulations. A= Section A, B= Section B, σ = yield stress, TCT = Total Component Thickness, NWZ= Number of Weakened Zones.

Case	Potential HIC_{15} prediction
TWB, A = 1.5 mm, B = 3 mm, σ = 400 MPa	1624.68
TWB, A= 3 mm, B= 1.5 mm, σ = 400 MPa	1685.5
TCT= 3 mm, σ = 400 MPa	1066.11
TCT= 2.5 mm, σ = 800 MPa	812.84
TCT= 3 mm, σ = 800 MPa	531.33
TCT= 3.5 mm, σ = 800 MPa	431.38
TCT= 3 mm, σ = 800 MPa, NWZ= 4	691.12
TCT= 3 mm, σ = 800 MPa, NWZ= 5	911.31
TCT= 3 mm, σ = 800 MPa, NWZ= 8	755.812

deceleration in the first phase of the impact and in the force on the retractor. The force on the retractor was fixed at 4500 N (the optimal value for the optimal pulse). The next step is to obtain the average deceleration in g's produced by the modified structure in the first phase, which allows obtaining the potential HIC_{15} using equation (4).

The results are shown in Table 4. It can be seen that, in general, modifications proposed with TWB style, generated predictions of a HIC_{15} potentially high. This comes from low deceleration in the first phase. It was observed that by increasing the thickness of the side rail member, the potential HIC_{15} was improved. By using 800 MPa of yield strength combined with 3 and 3.5 mm thick HIC_{15} best values were obtained. The introduction of crush initiators in the structure caused a weakened structure that produced low decelerations in the first phase of the crash, resulting in predictions of high HIC_{15} values.

7. REMARKS

To reduce HIC_{15}, high deceleration during the first phase of crash (first 18 ms) is desired, that is, a rigid front module is useful. However, the second phase of the crash requires low deceleration as discussed in the literature. These conditions present a real design challenge. From the previous design case, despite obtaining a good prediction of HIC_{15} (below 700) with the structural changes proposed for the first phase of crash, the design still must overcome the challenge of having a low deceleration level for the vehicle in the second phase of the crash. This is difficult to achieve because as the side rail members deform, the front module of the vehicle becomes more rigid (and starts contact with the engine) which could result in high decelerations. Under these conditions the reported optimal deceleration pulse would not be achieved. Some efforts have been proposed to control deceleration pulse through an active device. This active device should be able to absorb energy adapting the impact conditions (Witteman, 2005).

8. CONCLUSION

This paper presents a simplified model of the car deceleration pulse that can be used to evaluate the crashworthiness of a vehicle. In the model, the deceleration pulse is divided into 3 phases and each phase is assigned with a level of constant deceleration. Our results indicate that the error in the prediction of HIC_{15} produced by the model is small, compared to the results produced by the actual deceleration pulse. As mentioned, the model allows the introduction of the pulse deceleration shape as a design variable for the optimization of the restraint system.

Results of the simulations performed in this work show that the introduction of the deceleration pulse among the design variables of the restraint system, can reduce significantly the risk of injury, as measured by the HIC_{15} indicator. In particular, the design case presented here produced a combination of design parameters whose HIC_{15} indicator was reduced by 654 units with respect to the original design.

This article also introduced an equation obtained by the response surface method, which relates the value of the HIC_{15} indicator with specific design parameters during the first phase of the crash. A design case illustrated the use of this equation during the redesign of a structural component. In the proposed procedure, modification to structural components results in deceleration pulses that can be characterized by parameters of the simplified model of the deceleration pulse. The equation can then be used to predict HIC_{15} caused by the particular deceleration pulse. In this manner, the equation provides information that would otherwise be unavailable during the design stage. This new information can help the designer to make decisions about modifications to the structure of the car.

Future work includes studying the impact of the simplification of the crash pulse and its use as a design variable in a wide variety of crash scenarios. Also, better predictions can be obtained with the extension of the metamodel to take into account more variables like the second and third phase of the crash, and more variables of the occupant protection system.

REFERENCES

Cao, J. Z., Koka, M. R. and Law, S. E. (2004). Vehicle pulse shape optimization to improve occupant response in front impact. *CAE Methods for Vehicle Crashworthiness and Occupant Safety, and Safety-Critical Systems*. Warrendale, SAE, 71–77.

Chen, X. and Li, B. (2009). Crashworthiness and mass-reduction design of vehicles based on enhanced RSM. *5th IEEE Vehicle Power and Propulsion Conf.*, VPPC '09, Dearborn, MI, USA. 1755.

Consolazio, G. R., Chung, J. H. and Gurley, K. R. (2003). Impact simulation and full scale crash testing of a low profile concrete work zone barrier. *Computers and Structures* **81**, **13**, 1359–1374.

Du Bois, P., Chou, C. C., Fileta, B. B., Khalil, T. B., King, A. I., Mahmood, H. F., Mertz, H. J. and Wismans, J. (2004). Vehicle Crashworthiness and Occupant Protection. American Iron and Steel Institute. Southfield. Michigan. http://www.autosteel.org/~/media/Files/Autosteel/Research/Safety/safety_book.ashx

Eren, I., Gür, Y. and Aksoy, Z. (2009). Finite element analysis of collapse of front side rails with new types of crush initiators. *Int. J. Automotive Technology* **10**, **4**, 451–457.

EURONCAP (2011). http://www.euroncap.com/tests/frontimpact.aspx

Fang, H., Rais-Rohani, M., Liu, Z. and Horstemeyer, M. F. (2005). A comparative study of metamodeling methods for multiobjective crashworthiness optimization. *Computers and Structures* **83**, **25–26**, 2121–2136.

Goel, T. and Stander, N. (2009). Comparing three error criteria for selecting radial basis function network topology. *Computer Methods in Applied Mechanics and Engineering*, **198**, 27–29, 2137–2150.

Griffiths, M., Paine, M. and Haley, J. (1999). Consumer crash tests: the elusive best practice. *Symp. Worldwide Harmonization of Crash Test Programs*, Cologne, Germany. http://users.tpg.com.au/users/mpaine/ncap_tuv.html

Hamza, K. and Saitou, K. (2005). Vehicle crashworthiness design via a surrogate model ensemble and a co-evolutionary genetic algorithm. *Proc. ASME Int. Design Engineering Technical Conf. and Computers and Information in Engineering Conf.*, Long Beach, USA. 899.

Hamza, K. T. (2008). *Design for Vehicle Structural Crashworthiness via Crash Mode Matching*. Ph. D. Dissertation. The University of Michigan.

Hilmann, J., Paas, M., Haenschke, A. and Vietor, T. (2007). Automatic concept model generation for optimisation and robust design of passenger cars. *Advances in Engineering Software*, **38**, 11–12, 795–801.

Hu, S., Ma, Z.-D., Qi, C. and Hu, P. (2009). Magic cube approach application on crashworthiness design of front rail in front angle impact. *2009 IEEE Int. Conf. Mechatronics and Automation*, ICMA 2009, Changchun, China. 3521.

Huang, M. (2002). *Vehicle Crash Mechanics.* CRC Press. Boca Raton. Fla.

Insurance Institute for Highway Safety (2009). Frontal Offset Crashworthiness Evaluation Guidelines for Rating Injury Measures.

Kawabe, Y., Kondo, T., Masuda, D., Mogi, T., Obayashi, K. and Okabe, T. (2004). Restraint system optimization for dual test configurations of frontal crashes. *CAE Methods for Vehicle Crashworthiness and Occupant Safety, and Safety-Critical Systems*. Warrendale, SAE, 79–90.

Lee, S. I., Lee, D. C., Lee, J. I., Han, C. S. and Hedrick, K. (2007). Integrated process for structural-topological configuration design of weight-reduced vehicle components. *Finite Elements in Analysis and Design* **43**, **8**, 620–629.

Macey, S. and Wardle, G. (2009). *H-Point: The Fundamentals of Car Design & Packaging.* 1st edn. Design Studio Press (2009). Culver City. CA.

McHenry, B. G. (2004). *Head Injury Criterion and the ATB.* ATB User's Group. http://www.mchenrysoftware.com/HIC%20and%20the%20ATB.pdf

NCAC (2006). Finite Element Model of Dodge Neon. FHWA/NHTSA National Crash Analysis Center. Version 7. http://www.ncac.gwu.edu/vml/archive/ncac/vehicle/neon-0.7.pdf

NHTSA (2008). http://edocket.access.gpo.gov/cfr_2008/octqtr/pdf/49cfr571.208.pdf

Opiela, K. (2010). *Finite Element Model Archive*. http://www.ncac.gwu.edu/vml/models.html

Patel, N. M. (2007). *Crashworthiness Design using Topology Optimization*. Ph. D. Dissertation. University of Notre Dame.

Qi, C. (2008). *A Magic Cube Approach for Crashworthiness and Blast Protection Designs of Structural and Material Systems.* Ph. D. Dissertation. The University of Michigan.

Shi, Y., Zhu, P., Shen, L. and Lin, Z. (2007). Lightweight design of automotive front side rails with TWB concept. *Thin-Walled Structures* **45**, **1**, 8–14.

Solanki, K., Oglesby, D. L., Burton, C. L., Fang, H. and Horstemeyer, M. F. (2004). Crashworthiness simulations comparing PAM-CRASH and LS-DYNA. *CAE Methods for Vehicle Crashworthiness and Occupant Safety, and Safety-Critical Systems*. Warrendale, SAE, 11–19.

Witteman, W. (1999). *Improved Vehicle Crashworthiness Design by Control of the Energy Absorption for Different Collision Situations.* Technische Universiteit Eindhoven.

Witteman, W. (2005). Adaptive frontal structure design to achieve optimal deceleration pulses. *The 19th Int. Technical Conf. Enhanced Safety of Vehicles (ESV)*, Washington D.C., USA. NHTSA. 1–8.

Wu, H. and Xin, Y. (2009). Optimal design of the S-Rail for crashworthiness analysis. *Proc. 2009 Int. Joint Conf. Computational Sciences and Optimization*, *CSO 2009*, Sanya, Hainan, China. IEEE Computer Society 2009, 735.

Xu, T., Li, Y., Li, Q., Hao, L. and Song, W. (2010). Crashworthiness design of frontal rail using strain-energy-density and topology optimization approach. *3rd Int. Joint Conf. Computational Sciences and Optimization, CSO 2010: Theoretical Development and Engineering Practice*, Huangshan Mountain, Anhui, China. 24.

Yannaccone, J. R., Whitman, G. R. and Sicher, L. (2005). Pretensioners and injury risk. *Proc. - Annual SAFE Symp. Survival and Flight Equipment Association*, 63.